

[3] Dislocations in Ice and Deformation Mechanisms: from Single Crystals to Polar Ice

Maurine Montagnat and Paul Duval

LGGE/CNRS, BP96.38402
St Martin d'Hères cedex,
France

Keywords: Deformation, Dislocations, Ice, Polar Ice

Abstract. We present the main features of the plasticity of ice Ih: both monocrystalline and polycrystalline. The nature and dynamics of dislocations are analyzed, with emphasis being placed on the mechanical behavior of single crystals. The strong plastic anisotropy of the ice crystal is at the origin of the formation of strong strain heterogeneities within the polycrystal. Under the low-stress conditions of polar ice sheets, basal slip associated with the formation of orientation gradients is the main deformation mode. Lattice distortion promotes the formation of boundaries and continuous recrystallization.

Introduction

Dislocations are the main defects to be considered when dealing with plasticity in ice. The ice crystal has an hexagonal symmetry; theoretically permitting slip on basal and non-basal slip systems. However, plasticity in ice is governed by dislocation dynamics which are highly anisotropic at the crystal scale. Dislocations glide mainly on the basal plane, which is at the origin of strong strain heterogeneities between grains in a polycrystal. The rate-controlling processes in ice single crystals are still partly unknown as they are to be related to a flow law which is characterized by a stress exponent equal to 2. In the case of ice polycrystals, the deformation modes seem to change with stress level: the stress exponent is close to, or higher than, 3 for ice deformed in the laboratory (stresses greater than 0.1MPa), but drops to a value close to, or smaller than, 2 under ice sheet deformation conditions (strain rates as low as 10^{-12} s^{-1} , stresses lower than 0.1MPa).

Knowledge of the rheological properties of ice at low stresses is of great importance when modeling polar ice sheet flow. The purpose of this modeling is a better dating of deep ice cores as a way of understanding ice sheet – climate interactions. Note that there is no broad agreement concerning the rate-controlling processes. However, intracrystalline basal slip is accepted as being the dominant deformation process under the conditions prevailing in ice sheets.

This article presents the state-of-the-art concerning our knowledge of dislocation characteristics and behavior, and of deformation mechanisms in specimens ranging from single crystals to polar ice polycrystals.

Dislocations in ice single crystals

In an ice single crystal, according to dislocation self-energy, most common dislocations have one of the three Burgers vectors, $1/3 \langle 2\bar{1}\bar{1}0 \rangle$, and glide mainly on the basal plane [1,2]: see table 1. Rapid motion of short edge dislocation segments gliding on the $(10\bar{1}0)$ prismatic plane is observed by X-ray diffraction [3-8]. This non-basal glide appears to be an efficient process of basal dislocation generation, but does not significantly contribute to plastic deformation. However, it is worth noting that the dislocation sources are the surfaces for single crystal, and the grain boundaries for polycrystals. Dislocations with non-basal Burgers vectors $\langle 0001 \rangle$ and $1/3 \langle 11\bar{2}3 \rangle$ were

observed by X-ray topography [9]. Deformation induced by the slip of such non-basal dislocations on prismatic and pyramidal planes appears even more unlikely to occur as their number is very low. Dislocation motion in ice is closely related to the concentration of defects associated with proton disorder (Bjerrum defects) [10-11]. Based on proton disorder, several theories have been developed in order to simulate dislocation motion [8,12-13] and reveal that a larger concentration of Bjerrum defects near to the dislocation core would be required in order to explain the high dislocation mobility.

Type of dislocation	Burgers vector	Relative self-energy	Slip plane	Fault energy [mJ/m ²]	Extended width [nm]
Perfect	$1/3 \langle 11\bar{2}0 \rangle$	1	(0001) or $(10\bar{1}0)$	-	-
	$\langle 0001 \rangle$	2.7	$(10\bar{1}0)$		
	$1/3 \langle 11\bar{2}3 \rangle$	3.6	$(10\bar{1}1)$ or $(11\bar{2}2)$		
Partial	$1/3 \langle 10\bar{1}0 \rangle$	0.33	(0001)	~ 0.6	24 (screw) 47 (60°) 55 (edge)
	$1/3 \langle 0001 \rangle$	0.66	-	~ 0.9	>100
	$1/6 \langle 20\bar{2}3 \rangle$	1	-	~ 0.3	>400

Table 1. : Dislocations and slip systems in ice (from Hondoh [2])

Observation of dislocations in ice. The first observations of dislocations in ice were made by Hayes and Webb [14] using transmission X-ray diffraction topography and most of the following observations were obtained with this technique [7-8,15-18]. Transmission Electron Microscopy was also used, but this is limited by the difficulty of preparing thin specimens without initiating cracking, and by the rapid sublimation of the sample under the electron beam [19]. The etch-pit observations used to study dislocation motion in bulk ice can be questioned [16,19-20] as surface effects can affect the dislocation structure at more than 50 μm from the surface [17,18].

X-ray topography appears to be particularly suitable for ice [19] for several reasons. The absorption of X-rays by ice is low, allowing the study of thick samples (1-2 mm), the ice does not have to be studied under vacuum or at low temperatures, and the initial dislocation density in an artificially grown ice sample can be low enough ($\sim 10^6 \text{ m}^{-2}$) to be able to follow the motion of individual dislocations. Fig. 1 is a X-ray topograph showing basal dislocation loops with the $(\bar{1}100)$ diffraction plane. Important results have been obtained on dislocation dynamics by using synchrotron sources [15-16,21-22]. The high brightness of this X-ray source significantly reduces the exposure time, to less than one second, and allows *in situ* observations of dislocations. The use of a white X-ray beam is also a significant advantage as it allows the simultaneous observation of several diffracting planes, and several grains or sub-grains [23-24].

The main limitations of X-ray topography are the upper bound on dislocation density of about 10^9 m^{-2} and the spatial resolution being close to one micron; but still too high to detect partial dislocations.

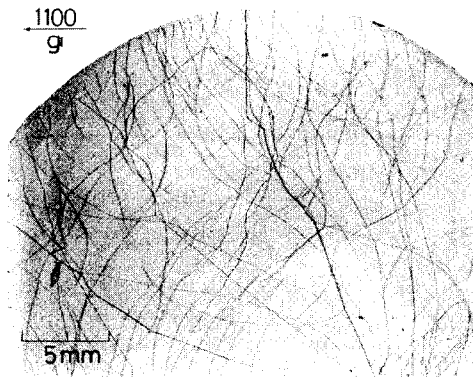


Fig. 1: X-ray topograph showing basal dislocation loops with the $(\bar{1}100)$ diffraction plane. From Higashi [9].

Dissociation of basal dislocations. Basal dislocations are known to dissociate into partial dislocations, separated by a stacking fault. The required conditions are satisfied when: $b^2 > b_1^2 + b_2^2$ and the stacking fault energy is sufficiently low, table 1. Stacking faults are mainly planar lattice defects lying on the basal plane and are associated with partial dislocations with $1/3 \langle 10\bar{1}0 \rangle$ Burgers vectors, Fig. 2. Faults with Burgers vectors of $1/2 \langle 0001 \rangle$ and $1/6 \langle 20\bar{2}3 \rangle$ were also observed [4,25]. The equilibrium separation between dissociated dislocations is about 20 nm for screw dislocations, and 55 nm for edge dislocations, which is very large when compared to other materials [2]. As mentioned earlier, the limited resolution of actual X-ray topographic techniques does not allow the observation of partial dislocations.

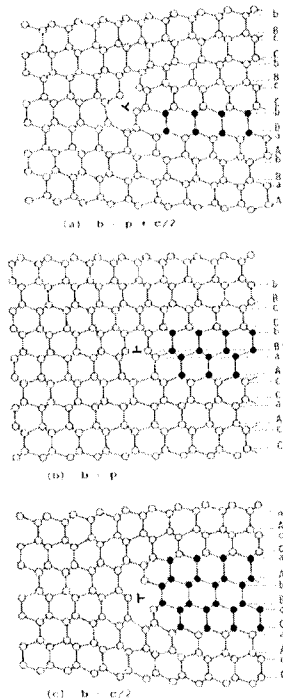


Fig. 2: Stacking faults lying on the basal plane associated with partial dislocations with the Burgers vector $1/3 \langle 10\bar{1}0 \rangle$. From Higashi [9]

Motion of dislocations. High quality measurements of dislocation velocities in single crystals were obtained by *in situ* X-ray diffraction topography [3,8,15,26]. The average velocity of dislocations on the basal plane varies linearly with the applied shear stress up to 1 MPa [27]. This linear dependence was also measured for edge dislocations slipping along the $(10\bar{1}0)$ prismatic plane [22]. The mobility of these non-basal edge dislocations is about five times higher than that of dislocations slipping on the basal plane, at a temperature of -10°C ; the difference increasing with decreasing temperature. This difference is well explained by the height of the Peierls barrier which is much lower for non-basal dislocations as compared to basal ones [22]. The activation energies, Q , for basal and non-basal dislocation mobility are given in table 2. A higher concentration of thermal kinks on the dissociated 60° dislocations would explain their larger mobility as compared to non-dissociated dislocations [26], table 2. The large difference between the values given by Shearwood *et al.* [8] and Okada *et al.* [26] is not explained [2]. This discrepancy is important regarding the physical mechanisms that control dislocation mobility.

	Q (eV)	Mobility ($\mu\text{m}\cdot\text{s}^{-1}\cdot\text{MPa}^{-1}$) at -20°C	
Basal screw	0.75	1.3	Okada <i>et al.</i> 1999 [26]
	0.95	1.0	Shearwood <i>et al.</i> 1991 [8]
Basal 60°	0.69	2.6	Okada <i>et al.</i> 1999
	0.87	2.0	Shearwood <i>et al.</i> 1991
Non-basal edge	0.61	14.5	Okada <i>et al.</i> 1999
	0.63	22.0	Shearwood <i>et al.</i> 1991

Table 2 : Mobility and activation energy (Q) of dislocations with $1/3 \langle 11\bar{2}0 \rangle$ Burgers vectors (from Hondoh [2]).

The dissociation of basal screw dislocations into two widely extended partial dislocations makes the cross-slip process in ice difficult, as constriction of these dislocations is required. However, Fukuda *et al.* [4] observed some cross-slip of basal screw dislocations onto a prismatic plane, by X-ray topography, and assumed that constriction occurred at the surface; thus creating edge dislocation segments that were mobile in the prismatic plane. Such constrictions may also occur at grain boundaries. The cross-slip of basal screw dislocations could explain the formation of basal slip bands from individual slip lines, as observed by Nakaya [28].

From the work of Hondoh [2], the climb mobility of dislocations in ice at -10°C is more than two orders of magnitude smaller than the mobility of dislocations gliding on the basal plane. The widely extended basal dislocations (with the stacking fault lying on the (0001) plane) restrict dislocation climb on the basal plane. Like cross-slip, dislocation climb is a very slow mechanism when compared with basal slip, but it should be involved in the formation of tilt-sub-boundaries composed of edge dislocations [4] and it could be the rate-limiting process in polycrystals deformed at high stresses (see below).

Deformation behavior of ice crystal

Creep experiments on ice single crystal are represented in Fig. 3 [11]. The creep behavior of an ice crystal is unusual in that the strain rate increases with time during primary creep; indicating dislocation multiplication [29]. A state of secondary or stationary creep is then reached. The density of mobile dislocations is constant, as a result of dislocation interactions between adjacent planes and

an equilibrium between dislocation creation and annihilation at the surface. The stress exponent of stationary creep is generally found to be 1.5-2.5 [27].

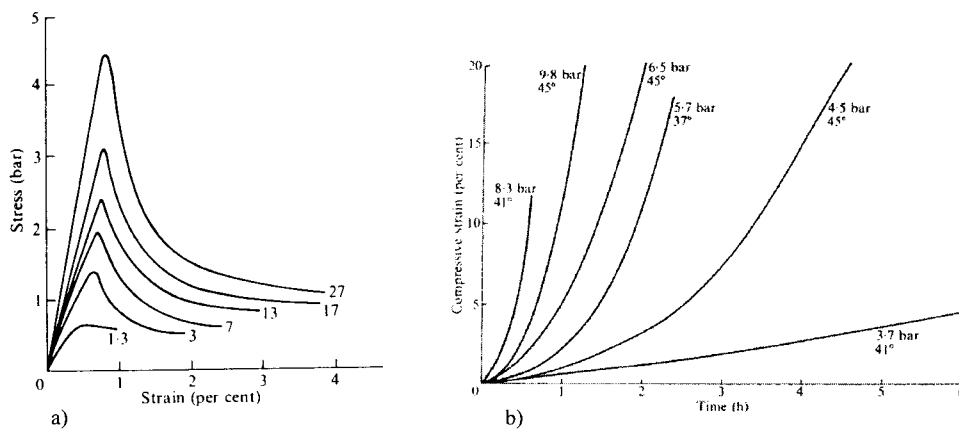


Fig. 3. : a) Compression tests at -15°C on ice single crystals for different strain rates ($\times 10^{-7} \text{ s}^{-1}$) [11]. *c*-axes were initially oriented at $45^{\circ} \pm 3^{\circ}$ from the compression axis.
b) Creep tests at -10°C . Stress values and *c*-axis orientations are indicated [11].

Ice crystal deformation occurs mainly by basal dislocation glide. Experiments done on badly oriented crystals revealed that the activation of non-basal glide systems requires a stress which is 60 times larger than that for the activation of basal glide [30]. However, the activation of non-basal systems is very difficult to achieve as the smallest misalignment of, or stress heterogeneity in, the sample induces a non-negligible amount of basal dislocation glide.

Strain gradient and geometrically necessary dislocations. When occurring under a strain gradient, plasticity can lead to the storage of geometrically necessary dislocations in addition to the storage of statistically stored dislocations resulting from chance encounters and reaction during the traffic of mobile dislocations [31-33]. The storage of geometrically necessary dislocations plays an essential role in the strengthening of materials and in the existence of an internal length scale during plasticity. Strain gradients can also be induced in polycrystals by the mismatch of slip at boundaries [32,34]. Strain gradients appear to be particularly influential in ice plasticity, due to the high viscoplastic anisotropy of the single crystal. The case of ice polycrystals will be developed later.

A torsion experiment induces a strain gradient along the radius and is therefore well-suited to characterising the response of the material to a strain gradient. These experiments were performed on artificially grown ice single crystals with low initial dislocation densities (less than 10^8 m^{-2}) [24]. Lattice distortions of the deformed sample were analysed by hard X-ray diffraction. The hard X-ray diffraction technique is a development of the original Laue technique that allows *in situ* observation of bulk samples, more than 1cm thick, using a white divergent beam in the high-energy range (100 – 400 keV) [35]. The resultant Bragg angles are low, and the diffraction patterns of several crystallographic planes can be observed simultaneously close to the direct beam. The orientation of the samples was chosen so as to align the torsion axis as closely as possible with the *c*-axis. The basal planes were then oriented for easy glide. The torsion creep curves obtained (Fig. 3) revealed no strain hardening up to 50% strain.

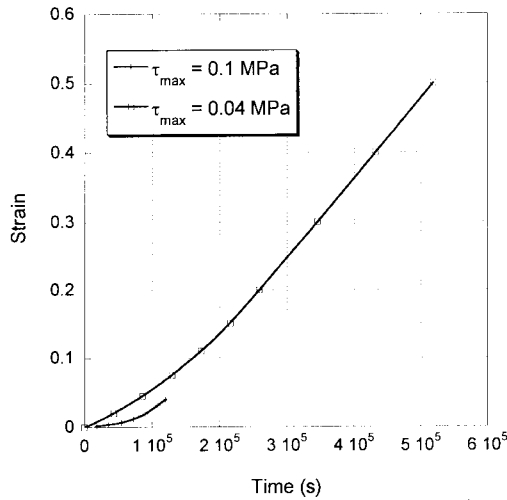


Fig. 4 : Torsion creep curves at -10°C , for a torsion shear strain of 0.1MPa and 0.04MPa.

Diffraction patterns (Fig. 5) reveal a distortion which is mainly associated with geometrically necessary dislocations [23-24,36], whose density is related to the measured lattice distortion around the Bragg angle by:

$$\rho_{geom} = \frac{\Delta\theta}{bD_e} \quad \text{eq. 1.}$$

where $\Delta\theta$ is the lattice distortion, b is the norm of the Burgers vector and D_e is the dimension of the sample over which the distortion is measured.

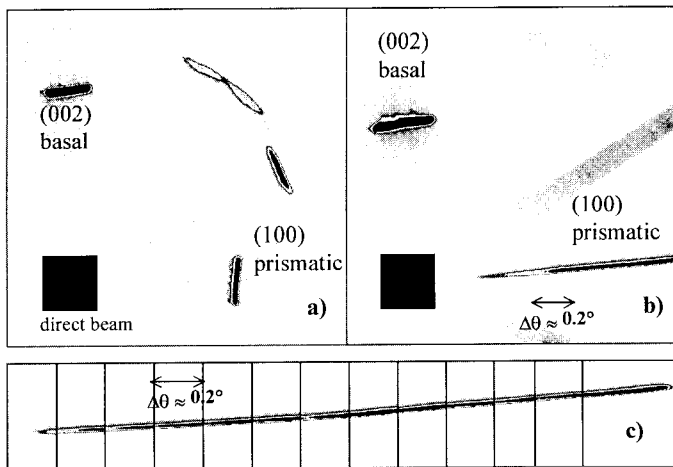


Fig. 5 : Diffraction pattern obtained for sample XR2. a) Diffraction pattern before deformation. The basal diffraction line is initially slightly distorted. b) Global diffraction pattern after deformation. Only one part of the distortion of the (100) diffraction line is shown. c) Reconstruction of the whole distortion of the (100) diffraction line by rotating the sample around the vertical axis. From Montagnat et al. [24]

The dislocations involved in the observed lattice distortion are mainly basal screw dislocations [24], which is consistent with the nature of the deformation.

It appears to be very clear that torsion strain is fully associated with geometrically necessary basal screw dislocations. Similar observations were made of a naturally deformed ice sample extracted from the Vostok ice core (Antarctica) as will be detailed later.

As no strain hardening was observed at up to 50% strain, the question of interactions between geometrically necessary dislocations remains open and could lead to an explanation of the low value of the stress exponent for the plastic deformation of ice single crystals.

Ice plasticity must then be analysed via mechanism-based theories of strain gradient plasticity.

Deformation mechanisms in ice polycrystals

The deformation behavior of an ice polycrystal is governed by the strong viscoplastic anisotropy at the crystal scale which induces strong deformation heterogeneities between grains. Dislocations are activated mainly on the basal plane, and grains can be “hard”, when badly oriented with respect to the applied stress, or “soft” when well oriented for glide on the basal plane. These strong heterogeneities are well illustrated by strain-rate comparisons between isotropic polycrystals and single crystals deformed under the same stress conditions, Fig. 6. The data concern the minimum creep rate reached. As a consequence of the strong single crystal anisotropy, the rate of deformation can be 4 orders of magnitude greater in a single crystal which is well-oriented for basal slip, than in an isotropic polycrystal [30], for the same applied stress. Strong heterogeneities develop at grain boundaries; thus inducing a strong kinematic hardening.

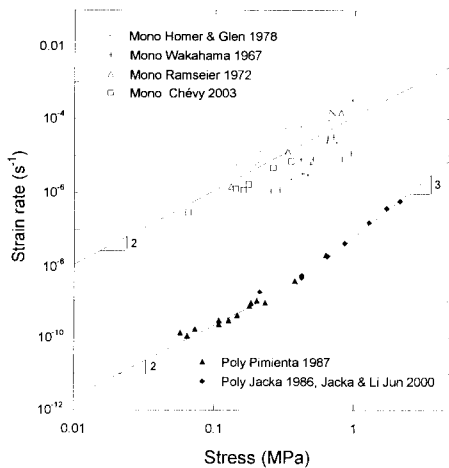


Fig. 6: Strain rate as a function of stress for the basal slip of an ice crystal and for isotropic polycrystalline ice [40-41,49-55]

Deformation at high stresses. When deformed at high stresses (between 0.1 and 2 MPa), an ice polycrystal is characterized by a flow law with a stress exponent that is close to 3. During primary creep, the strain rate decreases by more than 2 orders of magnitude (Fig. 7). On initial loading, the stress state within the polycrystalline ice sample is almost uniform. Deformation is essentially produced by basal slip. Because grain boundaries act as obstacles to dislocation slip, the resolved stress on the basal plane is relaxed by load transfer to harder slip systems [30]. As a result, an increasingly non-uniform state of internal stress develops, with peaks in amplitude near to grain boundaries. The initial creep rate is largely determined by basal slip systems; however, the steady strain rate is determined by an appropriate average over the resistance of all slip systems [37]. According to Hutchinson [38], extensive plasticity of polycrystalline ice is possible with four independent slip systems. Basal slip provides two independent systems. Slip or climb of dislocations on non-basal planes, as discussed above, would give additional independent systems

and these could constitute the rate-limiting processes that explain the stress exponent being equal to 3.

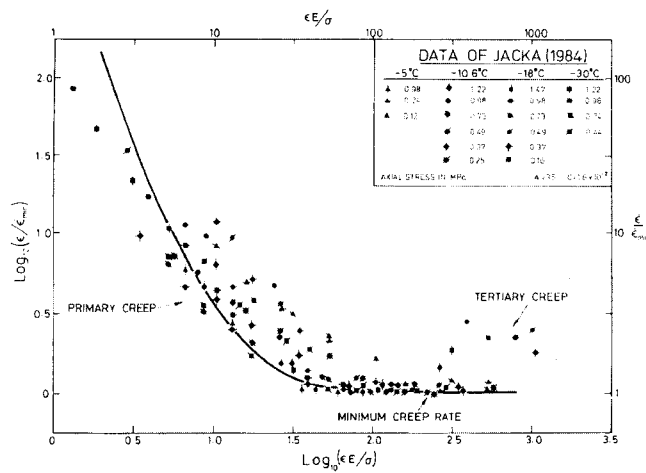


Fig. 7: Strain rate plotted against strain for isotropic polycrystalline ice using reduced variables (from Ashby and Duval [37]).

Fig. 8 presents creep curves for higher values of strain, where tertiary creep appears. Dynamic discontinuous recrystallization is then involved and the new grain boundary nucleation and migration together induce a softening which allows creep acceleration [39-40]. New grains are formed which are better oriented for basal slip, and equilibrium is reached between strain-induced hardening and softening associated with recrystallization mechanisms up to a steady-state tertiary creep. The grain size during dynamic recrystallization is primarily a function of stress [41].

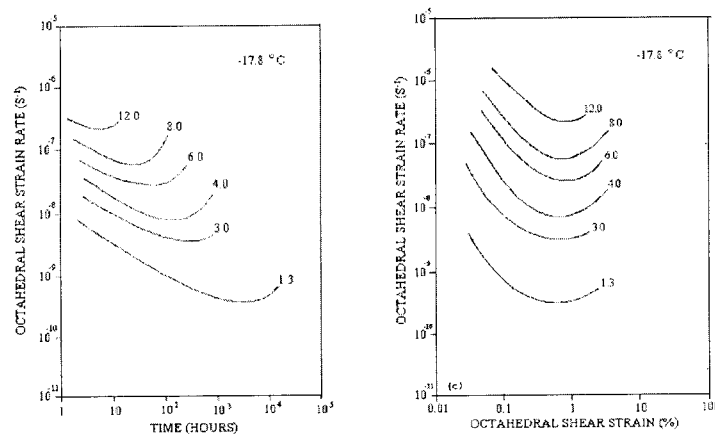


Fig. 8 : Creep curves for an ice polycrystal at -17.8°C and for different imposed stresses (in bars), from Jacka [40]

Viscous behavior of ice at low stresses; application to polar ice. For the conditions prevailing in ice sheets, (equivalent stress lower than 0.1 MPa), the stress exponent is slightly lower than 2; a value close to that found in isolated single crystals (Fig. 5). This result is supported by densification

measurements of bubbly ice at Vostok [42]. The Vostok ice core was drilled down to a depth of 3623 m in East Antarctica. The strain rate along the core is close to 10^{-13} s^{-1} , and the deviatoric stress is about 0.05 MPa [43]. As at high stresses, basal slip is the dominant deformation mode and other deformation modes are needed to ensure the compatibility of deformations at grain boundaries. However, the internal stress field induced by the incompatibility of the deformation between grains is reduced, under the low stress conditions of ice sheets, by grain boundary migration. Grain growth, driven by the free energy of grain boundaries, is observed in the first hundred meters of ice cores [44-49]. Continuous dynamic recrystallisation associated with the progressive misorientation of sub-boundaries is observed below the zone where normal grain growth occurs [48]. By sweeping away dislocations located in front of moving grain boundaries, grain boundary migration associated with grain growth and recrystallisation reduces the kinematic hardening induced by deformation incompatibilities between grains. Accommodation of slip by grain boundary migration in polar ice must be taken into account in order to explain the low stress exponent observed at low stresses.

Analysis of the microstructure of single crystals from the Vostok ice core (East Antarctica) by hard X-ray diffraction [36] has revealed a significant lattice distortion accommodated by geometrically necessary dislocations, as defined by Ashby [31]. Fig. 9 shows the diffraction pattern of an ice sample from a depth of 3516 m. The inclination of the (100) diffraction line is explained by torsion of the lattice around the *c*-axis whereas the inclination of the basal (002) line is due to bending of the basal plane.

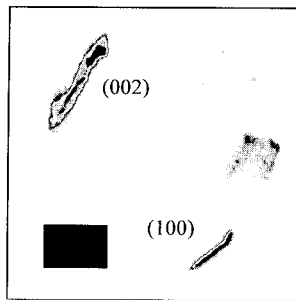


Fig. 9: Diffraction patterns for an ice sample from a depth of 3516 m along the Vostok ice core. Several crystallographic orientations are observed: the basal (002), prismatic (100) and several pyramidal planes. From Montagnat et al. [36].

The dislocation density associated with this lattice distortion is of the order of 10^9 m^{-2} . In comparison, the dislocation density of a “good” ice crystal, grown in the laboratory, is less than 10^8 m^{-2} . The dislocation density associated with statistically stored dislocations, as opposed to geometrically necessary ones, is observed to be generally low in Vostok samples [36]. It is important to point out that sub-boundaries and new grains should form as soon as the dislocation density exceeds a value of about 10^{10} m^{-2} . The distortion associated with geometrically necessary dislocations can explain the formation of sub-boundaries, as observed along the zone where continuous recrystallization occurs. A dislocation density higher than 10^{11} m^{-2} is expected in the depth range of 500 to 1500 m at Vostok, where sub-boundaries can be seen with the naked eye [48]. Sub-grains with misorientations of about 20° were observed at a depth of 2755 m by X-ray diffraction. The relatively low dislocation density at 3516 m is due to the high *in situ* temperature at this depth ($> -5^\circ\text{C}$) and the low horizontal shear stress caused by the presence of the lake below a depth of 3700 m [23]. The dislocation density, deduced from X-ray diffraction measurements, must be considered to be a lower bound since dislocations associated with pile-ups at grain boundaries could not be seen since only isolated ice crystals extracted from ice cores were studied. Note that grain boundary migration, by sweeping away dislocations located in front of grain boundaries,

should impede the formation of dislocation pile-ups in ice sheets. Most dislocations in deformed ice samples appear to be associated with strain gradients [36,49] and are geometrically necessary.

Rate-controlling processes in the creep of polar ice. The deformation of polar ice is essentially produced by dislocation slip on basal planes. The mismatch of slip at grain boundaries induces lattice distortion and strain gradients. Grain boundary migration associated with grain growth and recrystallisation reduces the dislocation density and the internal stress field. As a consequence, the strain rate is higher than that extrapolated from high stress conditions with a stress exponent of $n=3$. The large difference between the basal slip of single crystals and the creep behaviour of polycrystalline ice (Fig. 6) shows that the incompatibility of deformation between grains is significant even at low stresses. Mechanisms which give a value, for the stress exponent, of $n = 2$ at low stresses remain poorly known. The slowest deformation mechanism could control the strain rate if it occurs in series with basal slip. This is probably the case at high stresses, where non-basal slip or climb of dislocations should be the rate-controlling process. At low stresses, the number of these hard deformation systems is reduced by several processes, such as grain nucleation and grain boundary migration. With regard to non-basal slip, the bending of basal planes observed by hard X-ray diffraction must be taken into account when considering deformation along the *c*-axis. An analysis of dislocation microstructure by X-ray diffraction, made during the deformation of ice samples, will provide useful information on the level of internal stress field under low-stress conditions.

Conclusion

Ice plasticity is characterized by a strong viscoplastic anisotropy at the crystal scale, implying a strong anisotropy of deformation behaviour at the polycrystal scale. Dislocations glide mainly on the basal plane, and are dissociated into partials which complicate their movement onto other planes. The crystal deformation behaviour is characterized by a rapid dislocation multiplication followed by a stationary creep stage with no observed hardening. The origin of the stress exponent of 2 is still not well explained as far as the rate-limiting process is concerned. Strain gradients, when imposed by the shape of the solicitation, induce only the activation of geometrically necessary dislocations. Isotropic ice polycrystals deform much more slowly than do single crystal for the same imposed stress (by up to 4 orders of magnitude). Grains in polycrystals can be well-oriented for deformation or badly oriented, and strong heterogeneities are expected at grain boundaries. Under high-stress conditions ($\sigma > 0.1\text{MPa}$), the stress exponent is close to 3 and the rate-limiting factor should be associated with the activation of non-basal systems such as the climb of dislocations. Dynamic discontinuous recrystallization mechanisms appear soon after a deformation of 1%, allowing a softening by grain nucleation and fast grain-boundary migration. At the low stresses observed in polar ice sheets ($\sigma < 0.1\text{MPa}$), the stress exponent is closer to 2. Strong lattice distortions were measured and associated with a high density of geometrically necessary dislocations in natural ice samples. Together with the observed grain-boundary migration, these distortions seem to accommodate the high heterogeneities due to crystal anisotropy, and play a key role in dynamic continuous recrystallization mechanism (observed along the ice cores) by creating sub-boundaries. The climb of dislocations is necessary in order to explain the observed tilt sub-boundaries. However, the question of the rate-limiting processes remains to be explained in the case of the low-stress deformation conditions of ice sheets.

References

- [1] J.W. Glen and M.F. Perutz: *J. Glaciol.* Vol 2 (1954), pp 397-403
- [2] T. Hondoh, *Nature and behavior of dislocations in ice, Physics of Ice Core Records*, (Hokkaido University Press 2000), pp 3- 24.
- [3] A. Higashi, A. Fukuda, T. Hondoh, K. Goto, S. Amakai: *Proc. Yamada Conf. IX*, (University of Tokyo Press, Tokyo 1985), pp 511-515.
- [4] A. Fukuda, T. Hondoh, A. Higashi: *J. Phys. C1* 48 (1987), pp C1-163- C1-173.
- [5] S. Ahmad, R.W. Whitworth: *Phil. Mag. A* 57 (1988), pp 749-766.
- [6] A. Fukuda and A. Higashi: *Lattice defects in ice crystals* (Hokkaido University Press, Sapporo 1988), pp 69-96
- [7] C. Shearwood and R.W. Whitworth: *J. Glaciol.* Vol 35 n°120 (1989), pp 281-283
- [8] C. Shearwood and R.W. Whitworth: *Phil. Mag. A* Vol 64 (1991), pp 289-302
- [9] A. Higashi. *Lattice defects in ice crystals* (Hokkaido University press, Sapporo 1988)
- [10] J.W. Glen: *Physik des Kondensierten Mat.* Vol 7 (1968), pp 43-51
- [11] P.V. Hobbs: *Ice Physics* (Clarendon Press, Oxford 1974)
- [12] R.W. Whitworth, J.G. Paren and J.W. Glen: *Phil. Mag.* Vol 33 (1976), pp 409-426
- [13] H.J. Frost, D.J. Goodman and M.F. Ashby: *Phil. Mag.* Vol 33 (1976), pp 951-961
- [14] C.E. Hayes and W.W. Webb: *Science* Vol 147 (1965), pp 44-45
- [15] S. Ahmad and R.W. Whitworth: *Phil. Mag A* Vol 57 (1988), pp 749-766
- [16] F. Liu, I. Baker, G. Yao and M. Dudley: *J. Mat. Sci.* Vol 27 (1992), pp 2719-2725
- [17] F. Liu, I. Baker and M. Dudley: *Phil. Mag.* Vol 71 (1995), pp 1-14
- [18] F. Liu, I. Baker, G. Yao and M. Dudley: *Phil. Mag.* Vol 71 (1995), pp 15-42
- [19] I. Baker : *Micros. Res. Tech.* Vol 62 (2003), pp 70-82
- [20] S.J. Jones and N.K. Gilra : *Phil. Mag.* Vol 27 (1973), pp 457-472
- [21] S. Ahmad, M. Ohtomo and R.W. Whitworth: *Physics and chemistry of ice* (Hokkaido University Press 1986), pp 492-496
- [22] T. Hondoh, H. Iwamatsu and S. Mae: *Phil. Mag. A* Vol 62 (1990), pp 89-102
- [23] M. Montagnat, P. Duval, P. Bastie, B. Hamelin, O. Brissaud, M. de Angelis, J.R. Petit and V.Ya. Lipenkov: *C. R. Acad., Paris* Vol 333 (2001), pp 419-425.
- [24] M. Montagnat, P. Duval, P. Bastie and B. Hamelin: *Scripta Mater.* Vol 49 (2003),pp 411-415.
- [25] T. Hondoh, T. Itoh, S. Amakai, K. Goto and A. Higashi: *J. Phys. Chem.* Vol 87 (1983), pp 4040-4044
- [26] Y. Okada, T. Hondoh and S. Mae: *Phil. Mag. A* Vol 79 (1999), pp 2853-2868
- [27] V.F. Petrenko and R.W. Whitworth: *The physics of ice* (Oxford University Press 1999)
- [28] U. Nakaya: *US Army Snow Ice Permafrost Res. Estab. Res. Rep. n°28* (1958)
- [29] J.W. Glen: *Proc. Roy. Soc. London A* Vol 228 (1955), pp 519-538
- [30] P. Duval, M.F. Ashby and I. Anderman: *J. Phys. Chem.* Vol 87 (21) (1983), pp 4066-4074.

- [31] M.F. Ashby: *Phil. Mag.* 13 (1970), pp 399-424.
- [32] N.A. Fleck, G.M. Muller, M.F. Ashby and J.W. Hutchinson: *Acta Metall. Mater.* Vol 42 (1994), pp 475-487.
- [33] N.A. Fleck and J.W. Hutchinson: *J Mech Phys Solids* Vol 41 (1997), pp 1825.
- [34] V.P. Smyshlyaev and N.A. Fleck: *J. Mech. Phys. Solids* Vol 44 (4) (1996), pp 465-495.
- [35] Hamelin B, Bastie P. *J Phys IV France* Vol 8 (1998), pp 3-8.
- [36] M. Montagnat, P. Duval, P. Bastie, B. Hamelin and V. Ya. Lipenkov: *Earth Planet. Sci. Lett.* Vol 214 (2003), pp 369-378.
- [37] M.F. Ashby and P. Duval: *Cold Reg. Sci. Tech.* Vol 11 (1985), pp 285-300.
- [38] J.W. Hutchinson: *Metall. Trans.* Vol 8A (1977), pp 1465-1469.
- [39] P. Duval: *J. Glaciol.* Vol 27 (1981), pp 129-140
- [40] T.H. Jacka and M. Maccagnan: *Cold Reg. Sci. Tech.* Vol 8 (1984), pp 269-286
- [41] T.H. Jacka and J. Li: *Ann. Glaciol.* Vol 20 (1994), pp 13-18
- [42] V. Ya. Lipenkov, A.N. Salamatin and P. Duval: *J. Glaciol.* Vol 43 (1997), pp 397-407.
- [43] V. Ya. Lipenkov, N.I. Barkov, P. Duval and P. Pimienta: *J. Glaciol.* Vol 35 (121) (1989), pp 392-398
- [44] A. J. Gow and T. Williamson: *CRREL Rep.* 76-35, U.S. Army Cold Reg. Res. Eng. (1976)
- [45] P. Duval and C. Lorius: *Earth Planet. Sci. Lett.* Vol 48 (1980), pp 59-64.
- [46] T. Thorsteinsson, J. Kipfstuhl and H. Miller: *J. Geophys. Res.* Vol 102 (C12) (1997), pp 583-599.
- [47] A.J. Gow and 7 co-authors: *J. Geophys. Res.* Vol 102 (C12) (1997), pp 559-575.
- [48] S. de La Chapelle, O. Castelnau, V. Ya. Lipenkov and P. Duval: *J. Geophys. Res.* Vol 103 (B3) (1998), pp 5091-5105.
- [49] M. Montagnat and P. Duval: *C. R. Acad. Sci. Phys.* (2004) in press
- [50] J. Weiss, J. Vidot, M. Gay, L. Arnaud, P. Duval and J.R Petit: *Ann. Glaciol.* Vol 35 (2002), pp 552-558.
- [51] D.R. Homer, J.W. Glen: *J. of Glaciol.* Vol 21 (1978), pp 429-444.
- [52] G. Wakahama: *Physics of snow and ice* (Hokkaido University Press 1967), pp 291-311.
- [53] R.O. Ramseier, *Growth and mechanical properties of river and lake ice*, Ph.D. Thesis, Laval University, Canada (1972).
- [54] P. Pimienta, *Etude du comportement mécanique des glaces polycristallines aux faibles contraintes* Thèse de l'Université Joseph Fourier-Grenoble I (1987).
- [55] J. Chévy, personal communication.